MODELING CHARGE TRANSPORT IN AN ORGANIC SEMICONDUCTOR USING KINETIC MONTE CARLO METHODS

by

Brian Palmer II

A senior thesis submitted to the faculty of

Brigham Young University - Idaho

in partial fulfillment of the requirements for the degree of

Bachelor of Science

Department of Physics

Brigham Young University - Idaho

April 2026

BRIGHAM YOUNG UNIVERSITY - IDAHO

DEPARTMENT APPROVAL

of a senior thesis submitted by

Brian Palmer II

This thesis has been reviewed by the research advisor, research coordinator, and department chair and has been found to be satisfactory.

Date	Lance Nelson, Advisor
Date	Kevin Kelley, Committee Member
Date	Richard Hatt, Committee Member
Date	R. Todd Lines, Thesis Coordinator
Date	Evan Hansen, Department Chair

ABSTRACT

MODELING CHARGE TRANSPORT IN AN ORGANIC SEMICONDUCTOR USING KINETIC MONTE CARLO METHODS

Brian Palmer II

Department of Physics

Bachelor of Science

In this research, I refined a previously existing computational model to simulate charge dynamics in a donor–acceptor (DA) organic semiconductor system, and interpolated an overall trend of the system. Using a tight-binding Hamiltonian to represent the electronic structure and kinetic Monte Carlo (kMC) techniques to simulate stochastic hopping events, I investigated how molecular arrangement and coupling parameters influence charge mobility and energy relaxation. The simulations tracked thousands of charge trajectories across picosecond timescales and revealed key trends in energy distributions and spatial diffusion. These results offer insights into the mechanisms governing charge transfer efficiency in organic semiconductors and provide further foundation for computational modeling of organic materials in future photovoltaic devices.

ACKNOWLEDGMENTS

This research was funded by NSF REU Award PHY-2447841. I would like to thank Dr. Wai-Lun Chan for his mentorship, guidance, and insightful discussions throughout this project. I am also grateful to Dr. Stephanie Amos for her valuable support and contributions. Their expertise and encouragement have been instrumental in the development and success of this work. I would like to thank the BYUI Physics Department students and faculty for their friendship and support.

Contents

List of Figures

Chapter 1

Introduction

Silicon has long dominated commercial electronics due to its long-established fabrication infrastructure, high carrier mobility, and stability[1]. However, the growing demand for lightweight, flexible, and low-cost devices, particularly for wearables and medical sensors, has motivated the search for alternative materials[2]. Organic semiconductors are promising candidates for flexible optoelectronic applications because they can be processed at low temperatures, deposited on flexible substrates, and fabricated using scalable techniques[2].

Due to weak dielectric screening in organic semiconductors, photoexcitation generates bound excitons rather than free carriers. At donor–acceptor interfaces, these can form charge-transfer (CT) excitons with electrons and holes separated across the interface. Because their Coulomb binding energy (0.1–0.5 eV)[3] is higher than the thermal energy at room temperature, splitting into free carriers is inefficient. This means CT exciton separation creates a bottleneck in charge generation[4].

This work investigates charge transport in a donor–acceptor system composed of zinc phthalocyanine (ZnPc) and perfluorinated zinc phthalocyanine (F_8ZnPc), which form a model charge-transfer lattice[5]. A tight-binding Hamiltonian is used to de-

scribe the electronic structure, and kinetic Monte Carlo (kMC) simulations are used to model thermally-activated electron hopping. Two Hamiltonians are considered: a base model (BASE) and a modified model including added site potentials (AP). Together, they describe an eight-donor/eight-acceptor lattice.

The objective of this thesis is to study charge transport in this organic donor–acceptor system using tight-binding modeling and kMC simulations. Specifically, this work aims to:

- Extend the base tight-binding model by incorporating site potentials.
- Simulate thermally-activated hopping using kinetic Monte Carlo methods.
- Analyze how molecular energetics, coupling, organization energy, and separation affect transport.
- Compare transport behavior between the base and modified models.
- Provide physical insight into charge transport mechanisms in organic semiconductors.

Chapter 2

Methodology I: Potentials

Previous studies in modeling charge-transfer systems have relied heavily on numerical simulations to investigate how the arrangement of donor and acceptor molecules influences electronic properties. In our work, we adopted a Hamiltonian-based approach to model a simplified one-dimensional interface comprising donor and acceptor molecules. Donors host positively-charged holes and acceptors host negatively charged electrons. Each molecule is assigned a fixed position along the interface, and the Hamiltonian includes diagonal terms corresponding to Coulomb interactions between electron-hole pairs, as well as off-diagonal terms representing nearest-neighbor electronic couplings within donors and acceptors.

2.1 Previous Computational Models

The computational approach used in this study builds on the original MATLAB code developed by Dr. Wai-Lun Chan[5], which was designed to model the electronic structure of donor-acceptor interfaces. I translated this code into Python (Appendix A.1) to allow further analysis and expansion.

The eigenvalues and eigenvectors of the Hamiltonian provide insights into the system's electronic structure. Eigenvalues correspond to energy levels, while eigenvectors are used to determine the probability amplitudes of each charge configuration. The probability of finding the system in configuration $|i\rangle$ for a given eigenstate $|\psi\rangle$ is given by

$$P_i = |\langle i|\psi\rangle|^2 .$$

From these eigenvectors, we compute spatial-energy correlations using two approaches: (1) the average electron–hole distance weighted by the eigenstate probability, $\sum_i P_i \, r_i$, and (2) the difference between the weighted average positions of electrons and holes, $\langle x_e\rangle - \langle x_h\rangle$, where each expectation value is computed using the same probability weights P_i. Both approaches yield consistent results, allowing for a characterization of the spatial distribution of charge carriers.

Data visualization techniques such as scatter plots of average distance versus energy and histograms of eigenvalue distributions enable the identification of trends. This will be useful in seeing the effects of additional potentials on the system, which will be seen in this section. These plots provide insight into how the spatial configuration of molecules influences energy distributions and the localization of charge carriers (see Figures 2.1 and 2.2). This computational framework forms the foundation for analyzing the interplay between molecular arrangement and electronic behavior in our study.

2.2 Gaps in Current Computational Approaches

The original computational framework developed by Dr. Wai-Lun Chan provides a method for calculating the electronic structure of donor-acceptor interfaces. However, it assumes that all donor and acceptor sites are energetically equivalent aside

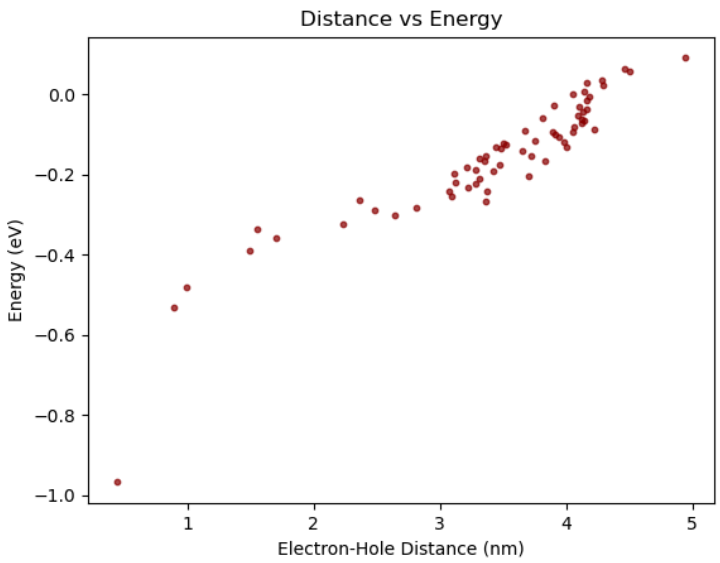

Figure 2.1: Scatter plot of average electron-hole distance versus eigenstate energy.

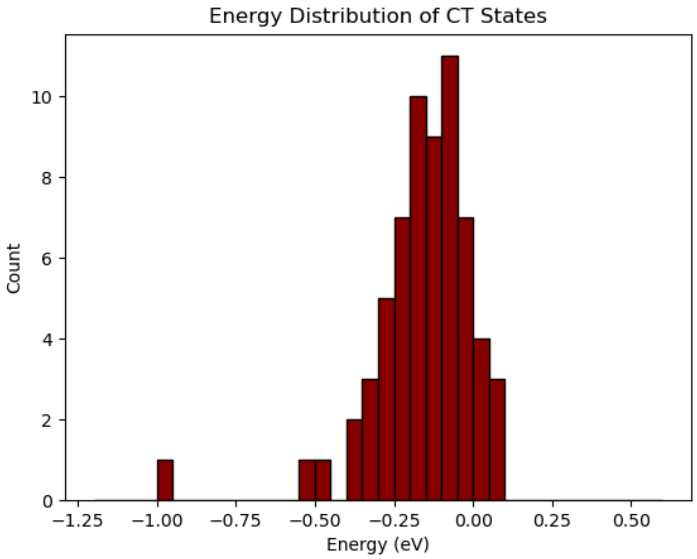

Figure 2.2: Histogram of eigenvalue distribution.

from the Coulomb interaction between electron-hole pairs. The diagonal elements of the Hamiltonian include only the Coulomb attraction, while the off-diagonal elements account for nearest-neighbor electronic coupling. This simplification neglects varia-

tions in site energies due to molecular arrangement, thus limiting the model's ability to capture the shifts in energy levels between molecules observed in real materials.

To address this gap, we incorporated site-specific potentials provided by Dr. Stephanie Amos[6], derived from atomistic calculations and visualized using the VESTA software package. VESTA (Visualization for Electronic and Structural Analysis) is a tool commonly used to analyze and visualize crystal structures, charge densities, and electrostatic potentials obtained from first-principles simulations. In this work, it was used to interpret potential data generated from density functional theory (DFT) calculations.

DFT is a quantum mechanical method used to compute the electronic structure of systems by solving for the ground-state electron density rather than the many-electron wavefunction. It provides a computationally efficient way to obtain quantities such as local electrostatic potentials and site energies in molecular and solid-state systems. The site-specific potentials used here originate from such DFT calculations, capturing how the local chemical environment modifies the energy landscape at each donor and acceptor site.

These potentials assign individual energy offsets to each donor and acceptor site, which are added to the diagonal terms of the Hamiltonian relative to the middle reference site. This modification allows the model to incorporate local energy disorder, leading to more realistic eigenvalue distributions and a more physically accurate representation of the system.

Figures 2.3 and 2.4 illustrate the impact of the added site potentials. In Figure 2.3, the scatter plot of average electron-hole distance versus eigenstate energy shows both the original results (BASE) and the results with site potentials overlaid (AP), showing shifts in energy levels and distances(Appendix A.1). Figure 2.4 presents the eigenvalue histograms for both cases, showing how the inclusion of site potentials redistributes

the population of charge-transfer states.

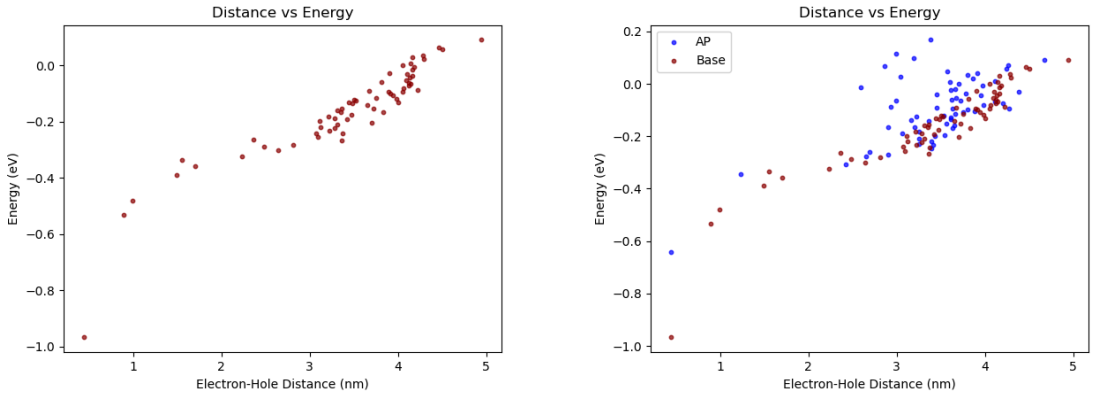

(a) Base model (b) With added site potentials

Figure 2.3: Comparison of average electron–hole distance versus eigenstate energy for the base model and the model including site potentials.

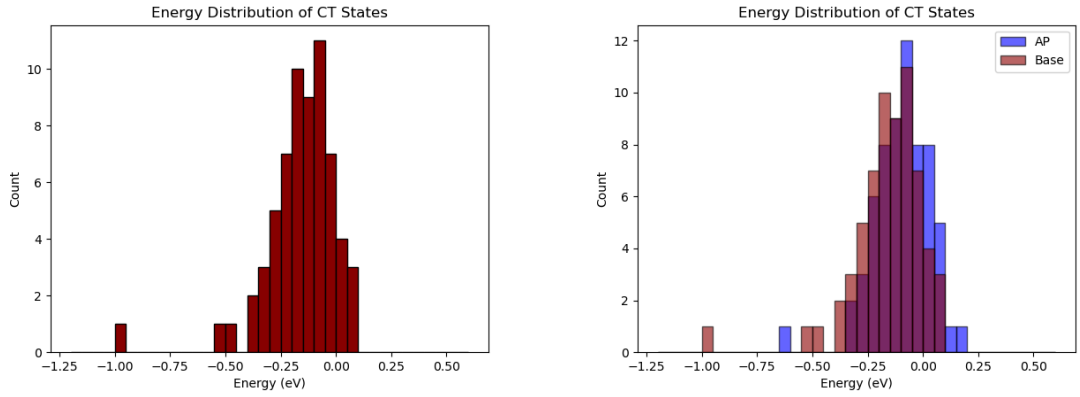

(a) Base model (b) With added site potentials

Figure 2.4: Comparison of eigenvalue distributions for both models.

The inclusion of site-specific potentials leads to a noticeable upward shift in the eigenvalue spectrum, reflecting an increase in energetic disorder within the system. This higher distribution indicates that charge configurations are no longer confined

to a narrow band of energies, but instead span a wider range due to local variations in the electrostatic environment. The observed differences between the base model and the model including site potentials are physically reasonable, given the changes introduced to the Hamiltonian. By adding site-specific energy offsets derived from DFT calculations, the system no longer assumes uniform energy across donor and acceptor sites. This naturally leads to a broader and more irregular energy landscape. As a result, eigenstates shift in energy and redistribute, producing both the upward shift and increased spread observed in the figures.

A key consequence of this increase is the emergence of higher-energy electron-hole pair states. These higher pair energies correspond to configurations in which the electron and hole occupy sites with elevated local potentials. Physically, this can be interpreted as the system accessing a larger set of energetically distinct configurations, increasing the density of available states at higher energies. Such states play an important role in charge separation, as they can facilitate transitions to more spatially separated configurations despite the Coulomb attraction between charges.

Additionally, the increased spread in eigenvalues enhances the correlation between energy and spatial separation observed in the system. Higher-energy states tend to correspond to more delocalized or spatially separated charge configurations. This effect is consistent with what we would expect with the introduction of local energy disorder, which disrupts uniformity and allows for a wider variety of charge distributions.

Overall, this chapter establishes a foundation for understanding how molecular arrangement and local site energetics influence the electronic behavior of donor–acceptor systems. These insights will be directly utilized in the next chapter, where the constructed energy landscape serves as the basis for the kinetic Monte Carlo simulation of charge transport.

Chapter 3

Methodology II: Monte Carlo Simulation

This chapter describes the construction and implementation of the kinetic Monte Carlo (kMC) simulation used to model charge transport in organic semiconductors. The goal of this simulation is to produce the stochastic dynamics of charge carriers undergoing thermally-activated hopping between sites, while incorporating the system's energetic and spatial configuration. The methods presented here form the computational foundation upon which all subsequent analysis and results in this work are based.

3.1 Model Formulation

The kMC model implemented in this work was constructed by extending the reference code provided by Dr. Chan[5]. The purpose of the model is to simulate charge transport through a network of electronic states. The system is defined by a discrete set of localized states indexed by $i = 1, \ldots, N$, where each state is characterized by

an energy E_i and a corresponding wavefunction expansion obtained from electronic structure calculations. These quantities are read directly from external data files and define the energy landscape through which the charge carrier evolves. The total number of states, N, is therefore determined entirely by the size of the input dataset, ensuring that the simulation directly reflects the underlying molecular system.

The spatial distributions of the lowest-energy eigenstate wavefunctions over the molecular lattice are compared in Figure 3.1 for the base potential (Appendix A.1) and added potential (Appendix A.1) cases, respectively. These distributions illustrate the degree of localization of the electronic states. The added site potentials broaden the localization and of the lowest eigenstates, thereby altering the connectivity of the lattice.

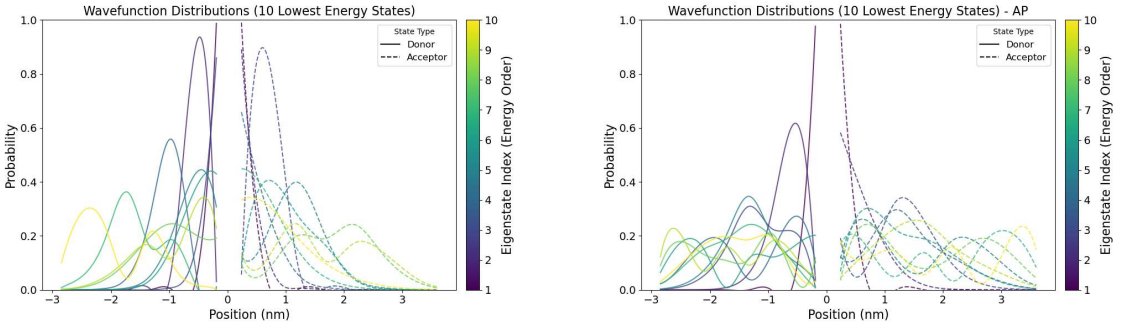

(a) Base potential

(b) With added site potentials

Figure 3.1: Comparison of wavefunction probability distributions for the base and added potential models.

As shown in Figure 3.2, the heat maps depict the charge-transfer state probabilities for both the base Hamiltonian and the Hamiltonian with added potential. Each subplot corresponds to a specific excited state, with donor sites along the vertical axis and acceptor sites along the horizontal axis. The comparison illustrates that

the added potential modifies the spatial distribution of the wavefunction, resulting in increased delocalization between donor-acceptor pairs.

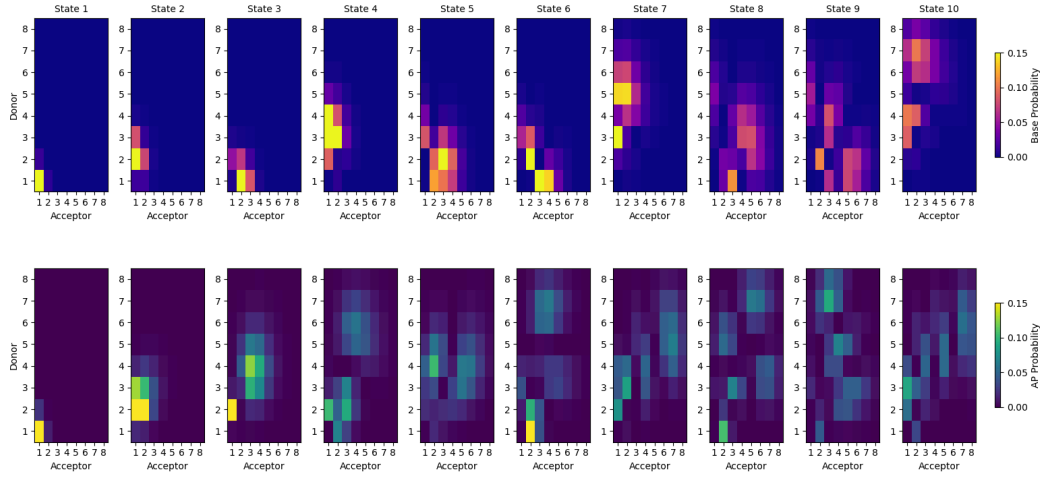

Figure 3.2: Wavefunction heatmap compares the distributions for the base and added potential models. Adding potentials increases the delocalization of the wavefunction.

Charge transport is modeled as a stochastic hopping process between pairs of states $i \to j$, with transition rates determined by three main contributions: (i) electronic coupling between states, (ii) thermal occupation, and (iii) phonon-assisted spectral weighting. The electronic overlap between states is quantified through the matrix

$$S_{ij} = \sum_k |V_{k,i}|^2 |V_{k,j}|^2, \tag{3.1}$$

where $V_{k,i}$ denotes the k-th component of the wavefunction associated with state i[7]. This overlap term captures the spatial and orbital compatibility between sites and serves as a proxy for electronic coupling strength.

3.2 Simulation Parameters and Assumptions

The kinetic Monte Carlo simulation requires the specification of several physical and numerical parameters that govern the charge transport dynamics. These parameters control the relative importance of thermal activation, vibrational coupling, and electronic disorder, and therefore determine the timescales and pathways explored by the charge carrier. The values used in this work were chosen to be physically reasonable for organic semiconductor systems and follow the reference framework developed by Dr. Chan[5].

In the simulation, the rate of hopping from state i to state j is computed as

$$k_{i\to j} = \frac{1}{\hbar}\, S_{ij}\, J_{ij}\, A_{ij}, \tag{3.2}$$

where $S_{ij} = \sum_k |V_{k,i}|^2 |V_{k,j}|^2$ captures the electronic overlap between states, J_{ij} is a spectral weighting term that can incorporate the effects of phonon-assisted transitions, and A_{ij} is a thermal factor derived from the Bose–Einstein distribution.

In this framework, the spectral term is written as the sum of two contributions: a low-energy reorganization component

$$J_{ij}^{(1)} = \lambda_1 \frac{\Delta E_{ij}}{\omega_c} \exp\Big(- \frac{\Delta E_{ij}}{\omega_c} \Big) \tag{3.3}$$

and a vibrational Lorentzian component

$$J_{ij}^{(2)} = \lambda_2 \frac{\gamma \Delta E_{ij}}{\pi[(\Delta E_{ij} - \hbar\omega)^2 + \gamma^2]}, \tag{3.4}$$

where $\Delta E_{ij} = |E_i - E_j|$, $\lambda_1 = 0.03$ eV and $\lambda_2 = 0.00$ eV are the reorganization energies, $\omega_c = 0.01$ eV is the cutoff energy for the exponential term, $\gamma = 0.02$ eV is the vibrational linewidth, and $\hbar\omega = 0.15$ eV is the vibrational mode energy.

This formulation allows for the inclusion of phonon-assisted transport through the Lorentzian term. However, in this work, we set $\lambda_2 = 0$, which removes this

contribution entirely. As a result, the dynamics are governed solely by the low-energy reorganization component $J_{ij}^{(1)}$. This allows us to isolate the baseline hopping mechanism and understand how transport behaves without vibrational resonance effects.

Thermal effects are incorporated through a fixed thermal energy scale $kT = 0.026$ eV, corresponding to room temperature. The thermal factor A_{ij} is implemented according to

$$A_{ij} = \begin{cases} \frac{1}{\exp[(E_j - E_i)/kT] - 1}, & E_j > E_i \\ 1 + \frac{1}{\exp[(E_i - E_j)/kT] - 1}, & E_j < E_i \\ 0, & i = j \end{cases}, \tag{3.5}$$

ensuring detailed balance and correct Boltzmann weighting. The total hopping rate out of each state is then summed over all target states, normalized, and used to generate stochastic trajectories in time. The Python code provided in Appendix A.1 implements these equations, constructs the cumulative probability distributions for each state, and iteratively propagates charge carriers through the system. By plotting multiple trajectories, we can visualize the ensemble of charge transport pathways and explore how local site energies and electronic structure influence the dynamics.

The kMC simulation was evolved for a maximum physical time of $T_{\max} = 50$ ps for each trajectory. An ensemble of $N_{\text{traj}} = 1000$ independent trajectories was generated to obtain meaningful results. Each trajectory represents the time evolution of a single charge carrier undergoing stochastic hopping between states. Averaging over many trajectories allows the overall transport behavior to be distinguished from individual trajectories.

The model has several simplifying assumptions. First, the simulation considers only a single charge carrier and therefore neglects carrier-carrier interactions, such as Coulomb repulsion. This approximation is valid in the low-density limit, where

transport is dominated by single-particle dynamics.

Second, the energetic disorder and electronic structure of the system are assumed to be static in time. That is, the molecular configuration and site energies do not evolve during the simulation. This corresponds to a quenched disorder approximation and is appropriate when the timescale of structural rearrangement is much longer than the timescale of charge transport.

Third, all hopping processes are assumed to be Markovian, meaning that each transition depends only on the current state of the system and not on its previous history. Memory effects and quantum dynamics are therefore neglected. This assumption is justified when environmental decoherence occurs on timescales much shorter than the hopping times, placing the system firmly in the incoherent transport regime.

Finally, the waiting time between hops is approximated by the inverse total escape rate, $\Delta t_i = 1/R_i$, rather than being sampled from an exponential distribution. This approximation significantly reduces computational cost.

Together, these parameter assumptions define a framework that captures the essential physics of thermally-activated charge hopping in disordered organic systems, while remaining simple and efficient to allow large trajectory simulations.

3.3 Numerical Methods

This section describes the numerical procedures used to implement the kinetic Monte Carlo model introduced in the previous chapter. While the previous formulation defines the transition rates and stochastic dynamics, the numerical methods determine how these equations are evaluated, sampled, and averaged. The simulation was implemented in Python using the `NumPy` and `Matplotlib` libraries, and is designed to efficiently generate large ensembles of trajectories, interpolate them onto

a common time grid, and compute meaningful observables.

3.3.1 Kinetic Monte Carlo Simulations

The kinetic Monte Carlo simulation proceeds by generating stochastic trajectories through the discrete state space defined by the Hamiltonian eigenstates. For each trajectory, the system is initialized in a fixed starting state and evolves through a sequence of hopping events until a maximum simulation time $T_{\max}$ is reached.

At each step, the current state i determines a set of transition probabilities P_{ij}, which are stored in cumulative form as

$$C_{ij} = \sum_{k \leq j} P_{ik}. \tag{3.6}$$

A uniformly distributed random number $\xi \in [0, 1)$ is drawn, and the next state j is selected such that

$$C_{i,j-1} \leq \xi < C_{ij}. \tag{3.7}$$

Basically, the interval from 0 to 1 is divided into segments whose sizes correspond to the transition probabilities. The random number determines which segment is selected, and therefore which state the system hops to. This method ensures that transitions occur with exactly the probabilities specified by the kMC model. Figure 3.3 illustrates the mechanics of the kMC algorithm. The lattice sites are represented as blue circles, with a vacancy highlighted in red. At each step, atoms adjacent to the vacancy are considered for hopping, as indicated by the green arrows, with the probability of each move determined by the system's transition rates. After a move is selected probabilistically, the vacancy updates to the new location, and the process repeats, capturing the stochastic evolution of the atomic configuration over time.

The physical time is incremented by the state-dependent waiting time

$$\Delta t_i = \frac{1}{R_i}, \tag{3.8}$$

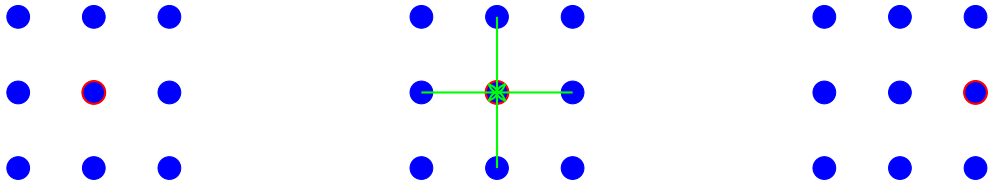

(a) Initial lattice with vacancy (red)

(b) Possible hops into vacancy

(c) After kMC selection: vacancy moves

Figure 3.3: Schematic of the kMC algorithm.

where R_i is the total outgoing rate from state i. This procedure generates a continuous-time stochastic-trajectory $\{E(t)\}$ describing the energy of the charge carrier as it hops through the energy landscape. Representative examples of individual stochastic trajectories are shown in Figure 3.4. Each curve corresponds to a single realization of the hopping dynamics, with some examples highlighted(Appendix A.1). The broad spread among trajectories reflects the intrinsic stochasticity of the kMC process and the presence of many possible relaxation pathways in the energy landscape.

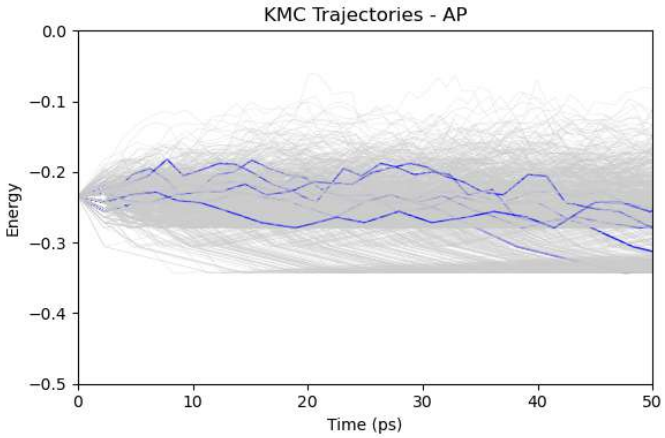

Figure 3.4: Example kinetic Monte Carlo trajectories.

An ensemble of $N_{\text{traj}} = 1000$ independent trajectories is generated in order to extract reliable transport behavior. Individual trajectories are stored and visualized,

while averaged quantities are computed through interpolation and averaging procedures described below.

3.3.2 Interpolation

Since each trajectory consists of hopping events occurring at irregular time intervals, averaging is not possible without mapping the trajectories onto a common time grid. To resolve this, each energy trajectory $E_n(t)$ is interpolated onto a fixed set of time bins,

$$t_k = k\Delta t, \quad k = 0, 1, \ldots, N_t, \tag{3.9}$$

where $\Delta t = 0.05$ ps and $t_{N_t} = T_{\max}$.

Linear interpolation is performed using

$$\tilde{E}_n(t_k) = \text{interp}(t_k; \{t_i, E_i\}), \tag{3.10}$$

where $\{t_i, E_i\}$ denotes the original irregularly sampled trajectory. The averaged energy is then computed as

$$\langle E(t_k) \rangle = \frac{1}{N(t_k)} \sum_{n=1}^{N_{\text{traj}}} \tilde{E}_n(t_k), \tag{3.11}$$

where $N(t_k)$ counts the number of samples contributing at time t_k. This procedure yields a smooth, continuous estimate of the mean energy relaxation dynamics.

3.3.3 Code Structure

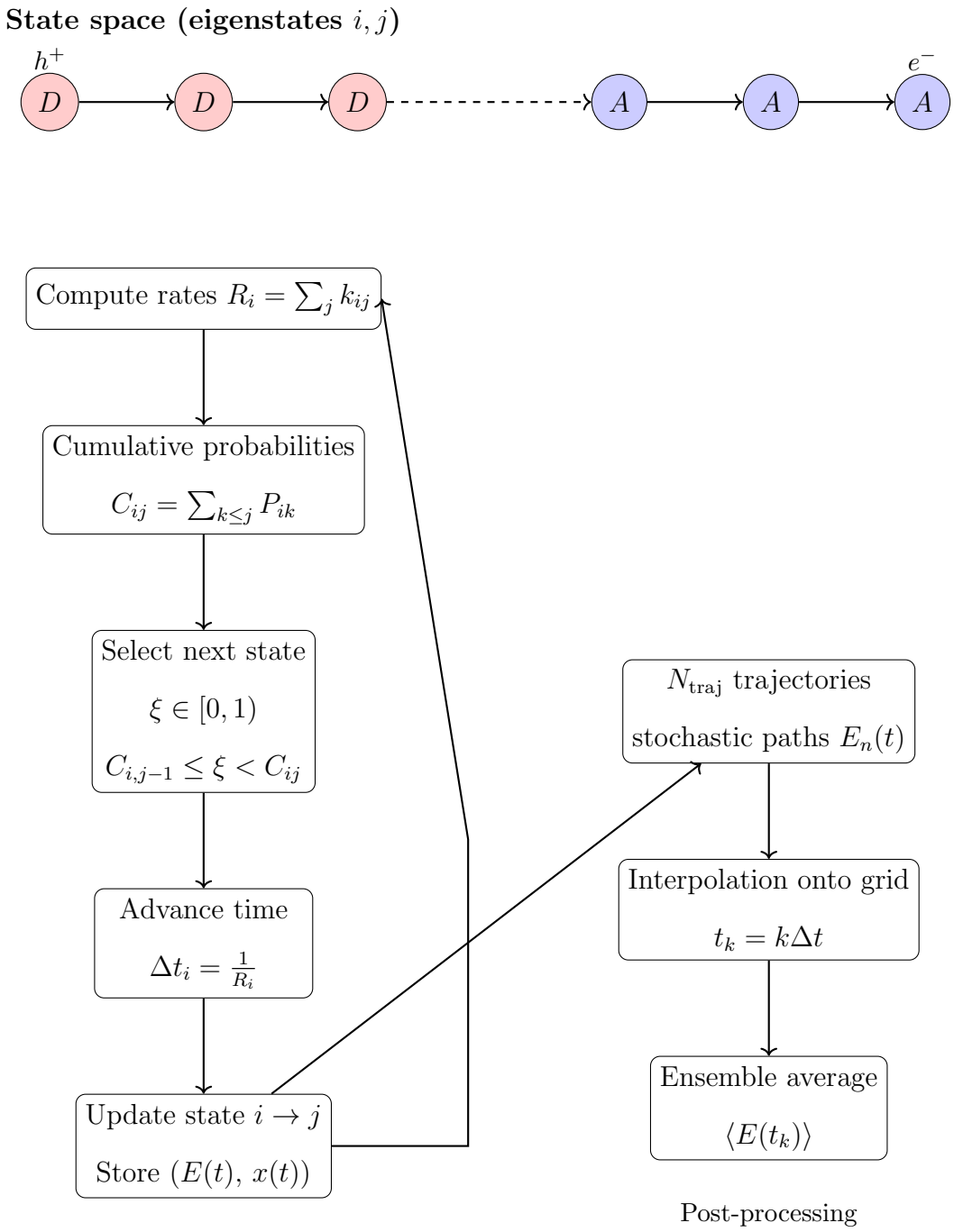

Figure 3.5: Schematic of the kinetic Monte Carlo (kMC) simulation.

Chapter 4

Results

This chapter presents the results obtained from the kinetic Monte Carlo simulations described in the previous chapters. Using the numerical framework, ensembles of stochastic trajectories were generated to investigate the energy relaxation dynamics of charge carriers in the donor-acceptor system. The focus of this chapter is on identifying trends in the time-dependent energy evolution and comparing behavior across different model configurations.

4.1 Observations from Kinetic Monte Carlo Simulations

The kinetic Monte Carlo simulations generate stochastic trajectories describing the time evolution of the charge carrier energy as it undergoes successive hopping events between localized states. Representative trajectories, along with the averaged energy, are shown in Figures. 4.1 and 4.2 for the base potential and added potential cases, respectively (Appendix A.1). In each figure, gray curves correspond to individual realizations of the stochastic process, while the highlighted curve represents the

average over all trajectories.

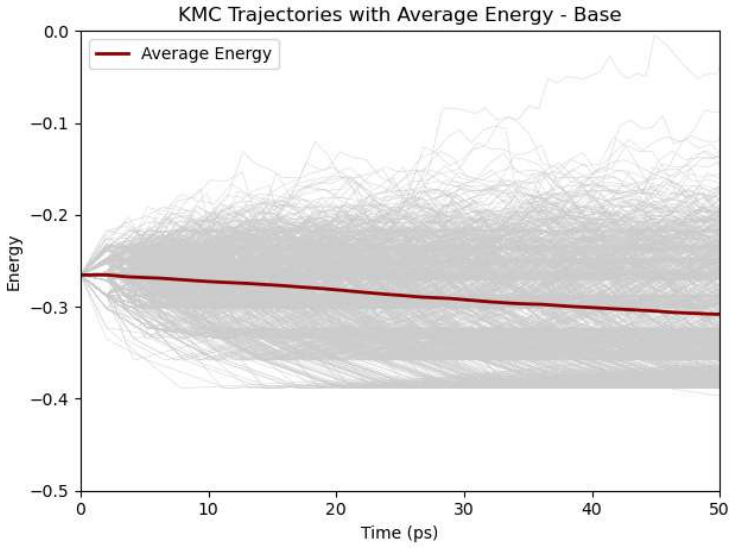

Figure 4.1: kinetic Monte Carlo trajectories for the base potential case.

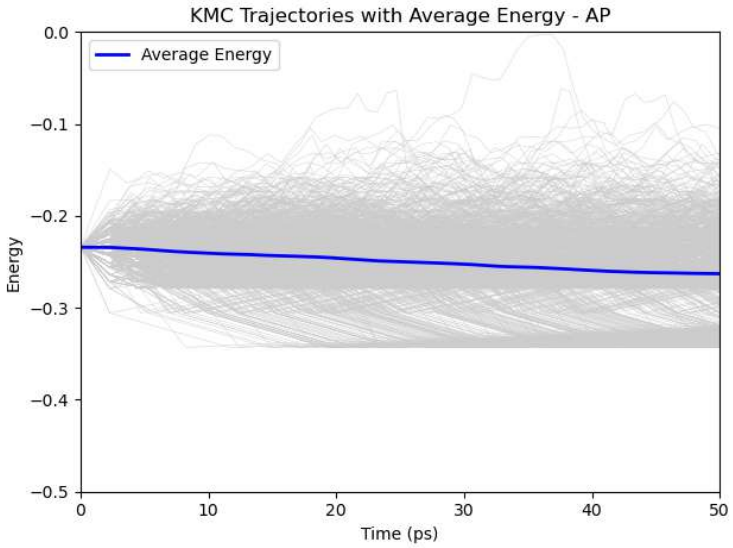

Figure 4.2: Representative kinetic Monte Carlo trajectories for the added potential case.

A key feature observed across all simulations is the decrease in carrier energy

at early times, followed by a slower relaxation toward a steady-state value. This behavior reflects the initial exploration of high-energy states, followed by progressive trapping in lower-energy regions of the energy landscape. The early-time regime is characterized by large energy fluctuations and frequent transitions, whereas the long-time regime exhibits smaller, less frequent energy changes.

Individual trajectories display significant variability, with some carriers rapidly descending into deep energy minima while others remain temporarily trapped in higher-energy configurations. This spread in behavior highlights the stochastic nature of the transport process and emphasizes the importance of averaging when extracting physically meaningful trends.

To directly compare the relaxation dynamics between the two models, the ensemble-averaged energy curves for the Base and Added Potential cases(Appendix A.1) are plotted together in Figure 4.3.

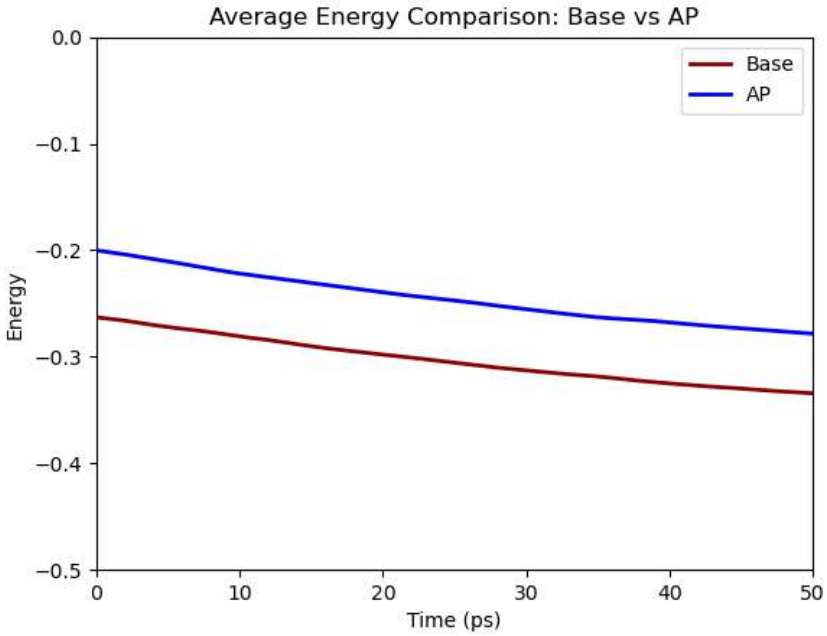

Figure 4.3: Comparison of ensemble-averaged energy trajectories for the base potential and added potential cases.

The averaged energy curves exhibit smooth decay, indicating that, on average, the system evolves toward increasingly stable configurations. The absence of unstable behavior in the average energy confirms that the system is undergoing irreversible relaxation. This is consistent with the underlying assumption of incoherent, thermally-activated hopping.

Additionally, the time scale over which the average energy approaches its steady-state value provides a direct measure of the characteristic relaxation time of the system. In the present simulations, the majority of the energy relaxation occurs within the first few picoseconds, after which the system enters a semi-stationary state dominated by rare transitions between the low-energy states.

Overall, these observations demonstrate that the kinetic Monte Carlo model captures the essential qualitative features of charge transport in donor-acceptor systems:

rapid initial relaxation, strong trajectory-to-trajectory variability, and slow long-time trapping dynamics. The comparison between the base and Added Potential cases further shows that microscopic modifications to the site energies can influence macroscopic relaxation behavior. These features form the basis for further analysis presented in the following sections.

4.2 Histogram Analysis for Energy Distribution

While individual trajectories and averaged curves provide insight into the evolution of the system, a different description can be obtained by examining the full distribution of carrier energies at fixed times. Histograms of the energy distribution were constructed by sampling the ensemble of kinetic Monte Carlo trajectories at selected time points.

Each stochastic trajectory was first interpolated onto a common time grid, allowing the carrier energy to be evaluated consistently across all realizations at any desired time. For a given sampling time t^*, the set

$$\{E_n(t^*)\}, \quad n = 1, \ldots, N_{\text{traj}}, \tag{4.1}$$

was extracted from the interpolated trajectories and used to construct a histogram representing the instantaneous energy distribution of the ensemble.

Representative histograms for both the Base potential and Added Potential cases. at $t = 5$ ps and $t = 50$ ps are shown in Figure 4.4. These four panels allow direct comparison of the statistical energy distributions across model configurations and time scales.

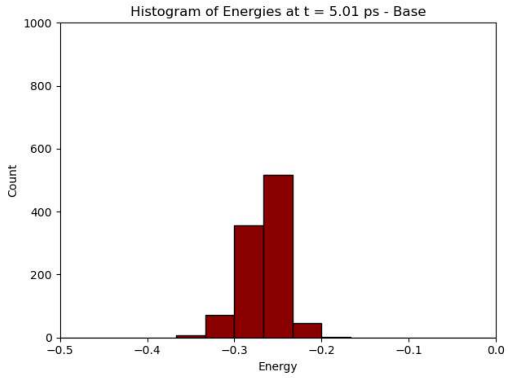

(a) Base potential, $t = 5$ ps

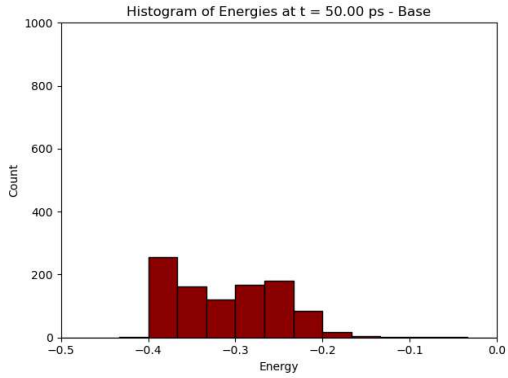

(b) Base potential, $t = 50$ ps

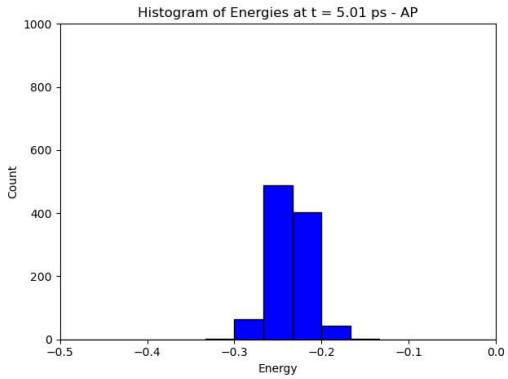

(c) Added potential, $t = 5$ ps

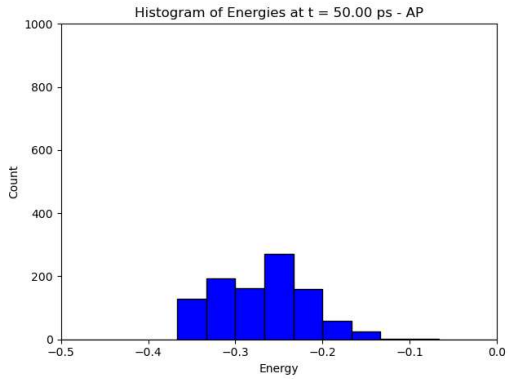

(d) Added potential, $t = 50$ ps

Figure 4.4: Histograms of carrier energy distributions for both the base and added potential cases.

At early times, the energy distributions are relatively narrow and sharply peaked, reflecting the fact that all carriers are initialized in similar energetic configurations. As time progresses, the distributions broaden and shift toward lower energies, indicating that the different stochastic trajectories go through unique relaxation pathways and populate a wider range of states.

The progressive broadening of the energy distributions reflects an increasing diversity of accessible configurations as carriers descend through the energy landscape. Rather than collapsing into a single dominant energy level, the ensemble spreads over

multiple low-energy states.

The downward shift of the distributions demonstrates systematic energetic relaxation, while the increasing width indicates that relaxation is not uniform across the ensemble. Some carriers rapidly reach deep low-energy states, while others remain in higher-energy configurations due to stochastic trapping and thermal activation.

The histogram analysis also reveals the non-Gaussian nature of the energy distributions, particularly at later times. The asymmetric shapes and extended tails toward lower energies suggest the presence of multiple relaxation channels and a broad spectrum of trapping depths, rather than simple exponential relaxation toward a unique equilibrium state.

Overall, the histogram-based analysis complements the trajectory-level observations by providing a different characterization of the energy landscape explored by the system. These distributions offer insight into the population dynamics of localized states and enable quantitative comparison between the Base and Added Potential models.

Chapter 5

Conclusion

In this thesis, a kinetic Monte Carlo framework was developed and implemented to investigate charge transport dynamics in organic donor-acceptor systems. Starting from electronic structure data generated by a Hamiltonian-based model, a stochastic simulation was constructed to resolve thermally-activated hopping events between localized electronic states. This approach enabled exploration of the relationship between microscopic energetic disorder, phonon-assisted transitions, and macroscopic transport behavior.

The numerical implementation was carefully formulated and validated through internal consistency checks, parameter sensitivity analysis, and convergence testing. Ensemble simulations revealed early-time energy relaxation followed by slower long-time trapping dynamics, consistent with theoretical expectations for incoherent charge transport in disordered organic materials. Individual stochastic trajectories exhibited strong variability, emphasizing the importance of averaging when extracting physically meaningful observables.

Histogram-based analysis further demonstrated that the energy distribution of charge carriers evolves in a non-Gaussian manner, with broad asymmetric distribu-

tions at intermediate times that gradually shift toward lower energies. These results highlight the role of energetic traps and multiple relaxation pathways in governing transport dynamics, and provide a more complete statistical characterization of the energy landscape explored by the system.

Beyond reproducing known qualitative features of charge hopping, this work establishes a computational framework that links electronic structure calculations to stochastic transport simulations. The modular structure of the code allows extension to more complex physical scenarios, including multi-carrier effects, dynamic disorder, and realistic phonon environments.

Overall, this thesis demonstrates that kinetic Monte Carlo methods provide a powerful tool for studying charge transport in disordered molecular systems. The framework developed here offers a foundation for future computational and experimental investigations aimed at understanding and optimizing transport processes in organic electronic materials.

Appendix A

Source Code

A.1 Code Availability

The code developed for this thesis is publicly available in the following GitHub repository:

`https://github.com/Queijobri/Brian-Palmer-Senior-Thesis-Code`

The repository is maintained by the author:

Palmer, Brian (2026). *Modeling Charge Transport in an Organic Semiconductor Using Tight-Binding and Kinetic Monte Carlo Methods*. GitHub repository.
`https://github.com/Queijobri/Brian-Palmer-Senior-Thesis-Code`

All code was written in Python and executed using standard scientific computing libraries, including NumPy, SciPy, and Matplotlib.

The repository serves as a complete and reproducible record of the computational methods used in this thesis.

Appendix B

Dr. Stephanie Amos Calculations

B.1 VESTA Energies

This Appendix contains the values calculated by Dr. Stephanie Amos and incorporated into the improved model.

The original image shows periodic site energies, which are a consequence of imposing periodic boundary conditions in the electrostatic calculation. The donor–acceptor interface is essentially repeated infinitely in space. As a result, each site feels not only the nearest interface but also its periodic images, producing a period of the electrostatic potential.

In a real device, however, the interface is not periodically replicated; it is bounded by a bulk donor on one side and bulk acceptor on the other. Therefore, the electrostatic potential should relax to constant values far from the interface. To reflect this, the site energies were manually constrained to plateau beyond a few lattice sites from the junction.

Values:

Donor Energies = -2.2374, -2.1212, -2.0632, -2.0438, -2.0438, -2.0438, -2.0438,

-2.0438

Acceptor Energies = -1.7244, -1.8019, -1.8502, -1.8599, -1.8599, -1.8599, -1.8599, -1.8599

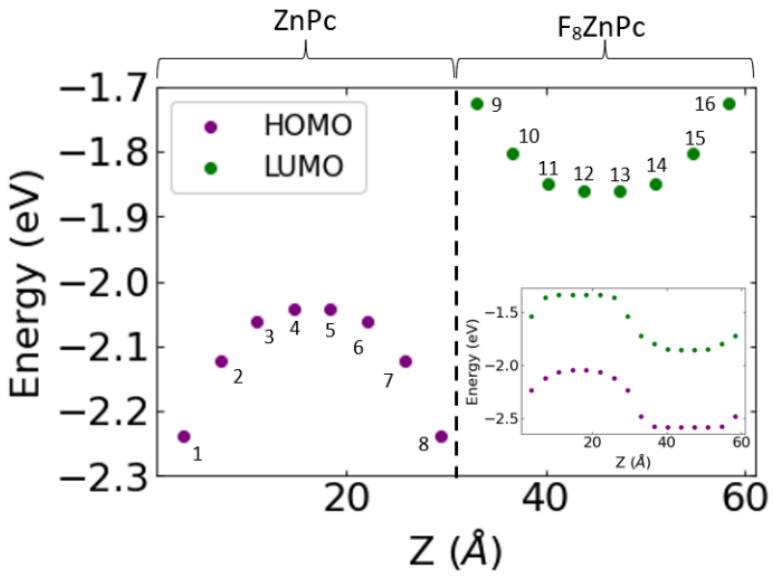

Figure B.1: VESTA figure showing periodic sight potentials for HOMO and LUMO bands

Bibliography

[1] Maciej Kamiński, Krystian Król, Norbert Kwietniewski, Marcin Myśliwiec, Mariusz Sochacki, Bartłomiej Stonio, Ryszard Kisiel, Agnieszka Martychowiec, Katarzyna Racka-Szmidt, Aleksander Werbowy, Jarosław Żelazko, Piotr Niedzielski, Jan Szmidt, and Andrzej Strójwas. The overview of silicon carbide technology: Status, challenges, key drivers, and product roadmap. *Materials (Basel)*, 18(1):12, 2024.

[2] M. Bouachrine and Sahbi Ayachi. Organic electronics: pioneering the future of sustainable and flexible technology. *RSC Advances*, 2025.

[3] Xiaoyang Zhu, Nicholas R. Monahan, Zizhou Gong, Haiming Zhu, Kristopher W. Williams, and Cory A. Nelson. Charge transfer excitons at van der waals interfaces. *Journal of the American Chemical Society*, 137(26):8313–8320, 2015.

[4] Jean-Luc Brédas, Joseph E. Norton, Jérôme Cornil, and Veaceslav Coropceanu. Molecular understanding of organic solar cells: the challenges. *Accounts of Chemical Research*, 42(11):1691–1699, 2009.

[5] Tika R. Kafle and Wai-Lun Chan. Exciton heating versus cooling: Charge separation driven by entropy and delocalization at interfaces with planar molecules. *Physical Review Applied*, 15:044054, 2021.

[6] Stephanie Amos. Personal communication. Conversation, June 3, 2025.

[7] Tika R. Kafle, Bhupal Kattel, Shanika Wanigasekara, Ti Wang, and Wai-Lun Chan. Spontaneous exciton dissociation at organic semiconductor interfaces facilitated by the orientation of the delocalized electron–hole wavefunction. *Advanced Energy Materials*, 10(10):1904013, 2020.